Lab on a Chip

Highly efficient combination of multiple single cells using deterministic single-cell combinatorial reactor

Journal:	*Lab on a Chip*
Manuscript ID	LC-ART-11-2024-000951.R1
Article Type:	Paper
Date Submitted by the Author:	07-Dec-2024
Complete List of Authors:	Yoshida, Mina; The University of Tokyo Institute of Industrial Science Tago, Saori; The University of Tokyo Institute of Industrial Science Iizuka, Kunihiko; The University of Tokyo Institute of Industrial Science; Lab Arco Limited Fujii, Teruo; The University of Tokyo Institute of Industrial Science Kim, Soo Hyeon; The University of Tokyo Institute of Industrial Science,

Highly efficient combination of multiple single cells using deterministic single-cell combinatorial reactor

Mina Yoshida[1], Saori Tago[1], Kunihiko Iizuka[1,2], Teruo Fujii[1] and Soo Hyeon Kim[1*]

[1] Institute of Industrial Science, University of Tokyo, Tokyo, Japan

[2] Lab Arco Limited, Osaka, Japan

Abstract

Compartmentalization of multiple single cells and/or single microbeads holds significant potential for advanced biological research including single-cell transcriptome analysis or cell-cell interactions. To ensure reliable analysis and prevent misinterpretation, it is essential to achieve highly efficient pairing or combining of single objects. In this paper, we introduce a novel microfluidic device coupled with a multilayer interconnect Si/SiO_2 control circuit, named the deterministic single-cell combinatorial reactor (DSCR) device, for the highly efficient combination of multiple single cells. The deterministic combination of multiple single cells is realized by sequentially introducing and trapping each cell population into designated trap-wells within each DSCR. These cell-sized trap-wells, created by etching the SiO_2 passivation layer, generate a highly localized electric field that facilitates deterministic single-cell trapping. The device's multilayer interconnection of electrodes enables the sequential operation of each trap-well, allowing precise trapping of each cell population into designated trap-wells within an array of combinatorial reactors. We demonstrated the feasibility of the DSCR by sequentially trapping three distinct groups of PC3 cells, each stained with a different fluorescent dye (blue, green, or red). This method achieved a 93 ± 2% pairing efficiency for two cell populations and an 82 ± 7% combination efficiency for three cell populations. Our innovative system offers promising applications for analyzing multiple cell-cell communications and combinatorial indexing of single cells.

Keywords: Single cell analysis, Cell trapping, Dielectrophoresis, Combination of particles, Si-SiO_2 device

Introduction

Single-cell analysis, which examines the properties and behaviors of individual cells, is widely utilized in both biology and medicine. Compartmentalization of multiple single cells and/or single microbeads is a crucial technology for enabling the single cell analysis. For instance, pairing a single cell with a single DNA barcoded-bead is utilized for indexing individual cells using DNA barcodes to perform comprehensive single-cell transcriptome analysis[1-3]. Single-cell transcriptome analysis is widely used to investigate the heterogeneity of cell populations and the discrimination of rare cells among large populations. Meanwhile, pairing different types of single cells is utilized to investigate cell-cell interactions at the single-cell level[4-6]. The interaction between two immune cells is investigated, and real-time monitoring of interactions is carried out at the single-cell level[7-11]. Although single-cell transcriptome analysis and cell-cell interactions have been successfully carried out, deterministic compartmentalization by improving the efficiency of pairing or combining single objects is highly required to acquire reliable analysis and prevent misinterpretation.

Efficient single-cell manipulation is an essential prerequisite for grouping different cell types at the single-cell level. Microfluidics is a promising technology for the efficient manipulation of single cells by utilizing cell-sized microstructures. Physical microstructures, microwells, and micro-holders are utilized for trapping only single cells using external forces, including gravity[12], hydrodynamic forces[13, 14], and dielectrophoresis (DEP)[15]. Water-in-oil droplet-based microfluidic devices are also widely used for the isolation of individual cells with tiny reactor volumes[16]. Droplet-based microfluidic devices utilize Poisson statistics to isolate single cells.

Recently, microfluidics-based single-cell manipulation methods have been widely utilized for pairing or compartmentalizing multiple single objects. Droplet-based microfluidics is one of the widely used methods for high-throughput and automated compartmentalization of multiple single cells[9, 17, 18]. Despite the widespread use of droplet platforms, a practical problem with pairing or combining is that the success ratio of pairing single cells is quite low with the statistical method, and this Poisson statistic should be overcome to improve the pairing or combination efficiency. Meanwhile, hydrodynamic forces and confined structures are widely used for the deterministic manipulation of single cells[19] and the pairing of multiple cells by utilizing micro-fabricated structures[20-25]. Gravity with cell-size microwells is also utilized for the pairing of cells[8, 26, 27]. Recently, dielectrophoresis (DEP) has been used for the manipulation of single cells and the pairing of single cells by inducing localized electric fields[28-30]. Physical

restriction with localized DEP forces is utilized for single-cell trapping and pairing by controlling multiple electrodes on the top and bottom surfaces of microfluidic devices, or two-pair interdigitated electrodes on a planar substrate.

Although previous systems were successfully used for pairing multiple single cells, the efficiency of the pairing should be improved, and the combination of different populations of single cells with more than three cells is difficult to achieve with previous systems. To realize the combination of multiple single cells, deterministic single-cell trapping and multiple microwells are required. Recently, we developed an electroactive microwell array for highly efficient deterministic single-cell trapping[31, 32]. The device was used for the analysis of intracellular materials of single cells and for the discrimination of each cell. However, the system was designed for single-cell trapping and cannot be used for pairing or combining multiple single cells. This is because the electrodes cannot be controlled individually. With the conventional microfabrication process, it is difficult to fabricate multilayer interconnected electrodes necessary for the individual control of electrodes. Previous research also tried to achieve individual control of electrodes for DEP trapping, but the maximum number of controllable electrodes would be three for the conventional photolithography technique used for the microfluidic device fabrication process.

Higher dimensions of controllability could be achieved by using multilayer interconnect Si/SiO_2 structure. Multilayer electrodes realized by using a SiO_2 insulation layer allow individual operation of electrodes. The multilayer interconnect Si/SiO_2 structure system is used for the manipulation of single cells by utilizing electrostatic manipulation of cells or liquids[33, 34]. For instance, DEP array was used for the manipulation of individual cells[35]. However, high-resolution single-cell trapping is required for the pairing of multiple single cells, which can be achieved by utilizing cell-sized physical restriction.

In this paper, we present a novel microfluidic device coupled with a multilayer interconnect Si/SiO_2 control circuit, named the deterministic single-cell combinatorial reactor (DSCR) device, for the highly efficient combination of multiple single cells. The deterministic combination of multiple single cells was achieved by sequentially introducing and trapping each cell population into designated trap-wells (Fig. 1). The tiny electrodes below the cell-sized trap-wells fabricated by etching the SiO_2 passivation layer induce a localized electric field inside the trap-wells, allowing highly efficient single-cell trapping. The multilayer interconnection of electrodes enables the sequential operation of each trap-well for trapping each population of cells into designated trap-wells located inside combinatorial reactors in an array. We report validation of the DSCR device by performing electric field simulation and evaluating the intrinsic single-

cell occupancy ratio of trap-wells by trapping prostate cancer cell line (PC3) cells. The feasibility of the DSCR for pairing and combining multiple populations of single cells was demonstrated by sequentially trapping three different groups of PC3 cells stained with blue, green, or red fluorescent dye.

Working principles and design of the device

Dielectrophoresis

Dielctrophoresis (DEP) is a phenomenon that dielectric objects move when it is immersed in a non-uniform electrical field. When a spherical cell with a radius of a is immersed in a non-uniform external electric field, $\boldsymbol{E}$, with a frequency, f, the DEP force ($\boldsymbol{F}_{DEP}$) acting on the cell can be approximated by

$$\boldsymbol{F}_{DEP} = 2\pi\varepsilon_e a^3 \mathrm{Re}[K(2\pi f)]\nabla|\boldsymbol{E}|^2 , \quad (1)$$

$$K(2\pi f) = \frac{\varepsilon^*_{\boldsymbol{cell}} - \varepsilon^*_{\boldsymbol{e}}}{\varepsilon^*_{\boldsymbol{cell}} + 2\varepsilon^*_{\boldsymbol{e}}} \quad (2)$$

$$\varepsilon^* = \varepsilon + \frac{\sigma}{2\pi f} j \quad (3)$$

where ε and σ are the electrical permittivity and the conductivity, subscripts *cell* and *e* represent cell and external medium, and $j = \sqrt{-1}$. The real part of the Clausius-Mossotti (CM) factor, $\mathrm{Re}[K(2\pi f)]$, express the relative polarization between the cells and the external medium. The sign of the real part of the CM factor determines the direction of dielectrophoretic movement; cells are attracted toward the strong electric field when $\mathrm{Re}[K(2\pi f)]$ is larger than 0 (positive DEP) and, conversely, cells are directed away from the strong electric field when the real part of the CM factor is less than 0 (negative DEP). In this study, positive DEP used for the manipulation of single cells, since highly localized electric field can be easily generated by using miniaturized electrodes. To induce strong positive DEP force a sucrose-based low conductivity buffer was used to decrease the conductivity of external medium. The sucrose-base low conductivity buffers were used for the demonstration of DEP manipulation and showed no effect on the cell viability during manipulation and cell culture after manipulation.

Design of the device

The deterministic single-cell combinatorial reactor (DSCR) device consists of a PDMS microfluidic channel for cell delivery and a silicon chip containing an array of combinatorial reactors (CR) for the combination of individual cells to isolate trapped cells from others and to prevent the release of trapped cells due to shear stress induced by bulk flow (Fig. 1B). Each CR (12 μm in height and 140 μm in diameter) contains three trap-wells: trap-well 1 (TW1), trap-well 2 (TW2), and trap-well 3 (TW3) (Fig. 1C). The distances between the trap-wells are each 70 μm, allowing them to be positioned within a combinatorial reactor. Each trap-well contains pair of electrodes 1 (E1), electrodes 2 (E2), or electrodes 3 (E3), respectively. The deterministic combination of three different cell populations is achieved by sequentially trapping each population into designated trap-wells.

Material and methods

Device fabrication

A silicon chip containing an array of combinatorial reactors was fabricated using the back-end of line (BEOL) process in CMOS IC fabrication (Supplementary Fig. S1). The silicon chip consisted of five metal wiring layers. The metal wiring was made of aluminum, and the insulating layer was made of SiO_2. By using multilayer metal wiring, the electrodes for DEP trapping were interconnected. After forming the DEP electrodes on the top metal layer, a passivation layer of SiO_2 was formed on the electrode layer to prevent leakage due to water. The thickness of the passivation layer was 5.6 μm. The trap-wells were fabricated by etching the SiO_2 passivation layer. After the fabrication of the trap-wells, a polyimide layer was coated on the passivation layer and etched to form CR.

The PDMS microfluidic channel was fabricated using conventional soft-lithography. A mold master was fabricated with a negative-type photoresist (SU-8 3035, MicroChem Co., USA). SU-8 3035 was spread onto a silicon wafer to achieve a thickness of 50 μm. The wafer was then soft-baked at 95°C for 15 minutes. A chromium photo-mask patterned for the fluidic channel was applied to the silicon wafer and exposed to ultraviolet light. The wafer was then post-exposure baked at 95°C for 5 minutes, and subsequently developed for 8 minutes using an SU-8 developer and rinsed with isopropyl alcohol. To allow for easy release of the PDMS replica, the mold master was exposed to CHF3 plasma and coated with a fluorocarbon layer using a reactive-ion etching machine (RIE-10NR; Samco Co., Japan). A PDMS prepolymer was mixed with a curing reagent (at a 10:1 mass ratio) and poured into the mold master. The mixture was incubated

in a desiccator at approximately 0.02 MPa for 30 minutes to remove bubbles from the PDMS prepolymer. Subsequently, the PDMS was cured at 75°C for 2 hours, and polymerized PDMS was then removed from the mold. The height and width of the microfluidic channel were 50 and 3,600 μm, respectively. Thereafter, holes were made to serve as access ports to the flow channels.

The silicon chip and PDMS microfluidic channel were exposed to O_2 plasma using a reactive-ion etching machine and bonded together. The SiO_2 passivation layer formed on the chip surfaces facilitates permanent bonding of the chip with PDMS microfluidic channels after oxygen plasma treatment. Before use, the device was washed with ethanol and water to prevent air bubbles in CRs and trap-wells; subsequently, the microfluidic channels were filled with a low conductivity buffer.

Cells and reagents

The PC3 human prostate cancer cell line (obtained from the RIKEN Bio Resource Center, Japan) was used for the demonstration. The PC3 cells were cultured in a humidified incubator (37°C in an atmosphere of 5% CO_2). The culture medium was RPMI 1640 (Invitrogen, USA) supplemented with fetal bovine serum (10%; Gemini Bio-products, USA) and penicillin-streptomycin (1%; Sigma Chemical Co., USA). To adjust the conductivity of the cell suspension medium, a low conductivity buffer (10 mM HEPES, 0.1 mM CaCl2, 59 mM D-glucose, and 236 mM sucrose) was used. Bovine serum albumin (BSA; Sigma Chemical Co., USA) was added to the low conductivity buffer to block nonspecific cell adhesion (0.6% w/v). The final conductivity of the low conductivity buffer was 8 mS m^{-1}.

Experimental setup

The device was placed on an x-y translational stage located on an upright microscope (MVX10; Olympus, Japan). Cells trapped in the device were monitored with a digital CCD camera (ORCA-R2; Hamamatsu Photonics, Japan) installed on the microscope. Electric potentials for DEP trapping and EP lysis were applied to the ITO electrodes using a function generator (WF1948; NF Corp., Japan) through an amplifier (HSA4101; NF Corp., Japan). Gastight glass syringes (Hamilton Company, USA), connected to the outlet of the microfluidic device, were mounted on precisely controlled syringe pumps (MFS-SP1; Microfluidic System Works Inc., Japan).

Cell trapping

Cultured PC3 cells were stained with a blue fluorescent probe (CellTracker Blue CMAC;

Invitrogen, USA), a green fluorescent probe (Calcein AM; Wako Pure Chemical Industries Ltd., Japan), or a red fluorescent probe (CellTrace™ Calcein Red-Orange, AM; Invitrogen, USA). Before cells were injected into the device, the culture medium was gently removed following centrifugation at 190 × g for 3 minutes, and the low conductivity buffer was added to adjust the conductivity of the cell suspension medium to induce positive DEP. A wide range of cell concentrations, from 2.7×10^4 to 2.2×10^5 cells mL^{-1}, was used for the demonstration. Cells were delivered into the microfluidic channel by withdrawing a syringe plunger, where the syringe is connected to the outlet of the microfluidic device. Cells were trapped in the trap-wells by applying electric potentials to the electrodes. Fluorescence images of the well array were acquired, and trapped cells were counted.

Results and discussion

Addressable electroactive trap-well array on Si/SiO_2 structure

Multilayer interconnections in the Si/SiO_2 structure enable precise control of individual electrodes within the trap-wells. This addressable electroactive trap-well array facilitates the selective trapping or release of single cells. To demonstrate the feasibility of using the Si/SiO_2 structure for precise single-cell manipulation, a single SiO_2 trap-well was fabricated in a reactor (Fig. 2A), where each electrode was individually controlled by transistors. Thin trap-wells (4 μm in height and 22 μm in diameter) were fabricated by etching the SiO_2 passivation layer to achieve single-cell resolution during DEP trapping, and each trap-well was aligned with the pair of electrodes (Fig. 2B). The pair electrodes located below each trap-well induce highly localized electric fields for single-cell trapping using DEP. The distance between electrodes was 8 μm, which was smaller than the target cell diameter (15 μm). The thickness of the SiO_2 passivation layer between the electrode and the bottom surface of the trap-well was 1.6 μm. Figure 2C shows the comparison of the simulated electric field distribution and vectors of the electric field gradient ($\nabla|\boldsymbol{E}|^2$) between the device without trap-well and with trap-well. The trap-well fabricated by etching SiO_2 passivation layer enables the formation of highly localized and high magnitude of $\nabla|\boldsymbol{E}|^2$ through the thin SiO_2 layer at the high-frequency regime (8 MHz), inducing strong DEP forces for cell trapping. Moreover, this cell-sized trap-wells restrict available space for the accommodation of a cell; only one cell can be trapped in a trap-well.

The selective trapping capability was demonstrated by capturing PC3 cells in designated SiO_2 trap-wells. These cells, stained with Calcein, were introduced into the device through an inlet and flowed through the microfluidic channel. Cells flowing over the activated trap-wells were efficiently captured by DEP when an electrical potential of 10 Vpp at 8 MHz was applied to the selected wells (Supplementary Movie 1 and Fig. 2D). However, cells flowing over deactivated wells were not trapped. The trapped cells emitted a clear fluorescence signal of Calcein with no change in fluorescence intensity observed, indicating an intact cell membrane during cell trapping using the SiO_2 trap-wells. The high frequency of 8 MHz was selected for DEP trapping, as this frequency minimizes the induction of transmembrane potential on the cell membrane, reducing potential damage to the membrane while maximizing DEP force (Supplementary Fig. S2).

Selective release of trapped cells was demonstrated by deactivating specific trap-wells within the array. After trapping PC3 cells by activating all trap-wells with an electrical potential of 10 Vpp at 8 MHz, single cells in selected trap-wells were released by deactivating the

corresponding trap-wells (Supplementary Movie 2 and Fig. 2E). When deactivated, the cells in those trap-wells were immediately released due to shear stress from the bulk fluid flow in the microfluidic device. However, cells in still-activated trap-wells were not released, as the localized DEP force continued to hold them securely in place. Proper surface treatment is crucial to ensure effective cell release and prevent nonspecific binding to the trap well surface. This result indicates that the SiO_2 trap-wells, fabricated by etching the SiO_2 passivation layer, allow highly localized and controllable manipulation of single cells. There is no interference between the electric fields of adjacent trap-wells, as the pair of electrodes were fabricated at the bottom of each trap-well and the SiO_2 layer effectively passivates the electric fields induced by the electrodes. The multilayer interconnections enable highly precise control of the electrodes through individual transistors.

Previous research utilizing microelectrode array (MEA) demonstrated the manipulation of single cells using DEP by controlling individual electrodes[36, 37]. In these approaches, the MEA was patterned on the bottom surface of the microfluidic channel, with a planar counter-electrode positioned on the ceiling of the channel. Although the system enables precise manipulation of a single cell using DEP, this configuration could cause the electric field to form throughout the entire microfluidic channel, leading to the unintended trapping of multiple cells simultaneously. Additionally, since the system relied on a single counter-electrode on the ceiling of the microfluidic channel, the electric field distribution varied when some MEA electrodes were deactivated. Furthermore, the scalability of the controllable electrodes was limited because all electrodes were fabricated on the same layer. In contrast, the Si/SiO_2 structure offers significant advantages in terms of scalability and controllability. By patterning electrodes on different layers, the system allows for straightforward expansion of the controllable electrode array. Moreover, the pair of electrodes fabricated at the bottom of each SiO_2 trap-well generates a highly localized electric field, enabling precise single-cell trapping with high resolution. This physical SiO_2 structure ensures stable single-cell trapping and eliminates interference between the electric fields of adjacent trap-wells.

The microfluidics on Si/SiO_2 structure demonstrates highly precise manipulation of single cells, enabling selective trapping and release of cells at the single-cell level. The multilayer interconnections and transistor-based control of each electrode offer significant advantages for single-cell manipulation. The electric field, highly localized within the SiO_2 trap-wells, ensured that cells were only trapped when the electrical potentials were applied to the individual SiO_2 trap-wells. Furthermore, once the single cells were trapped into the trap-wells, a second cell

cannot be trapped into the same trap-wells because the size of the microwells (22 μm) is comparable with that of the target cells; there is no available space for a second cell trapping. These results represent a unique feature of the microfluidic device, which is implemented on a Si/SiO_2 structure.

Deterministic single cell trapping using deterministic single-cell combinatorial reactor

The deterministic single-cell combinatorial reactor (DSCR) device consists of a PDMS microfluidic channel for cell delivery and a silicon chip containing an array of combinatorial reactors (CRs), where each CR contains three addressable SiO_2 trap-wells for deterministic single-cell trapping (Fig. 3A and 3B). The multilayer-interconnected electrodes of each trap well in a CR can be controlled independently (Fig. 3C), allowing sequential operation of trap-wells for the combination of single cells.

The deterministic single-cell trapping using DSCR was demonstrated by trapping single PC3 cells into SiO_2 trap-wells. The PC3 cells stained with Calcein (green fluorescent dye) were loaded onto the inlet of the device and delivered to the microfluidic channel at a flow rate of 4 μL min^{-1}. Electrical potential was applied to the electrodes at the bottom of TW1, and the PC3 cells were trapped into TW1 (Fig. 3D and Supplementary Movie 3). Single cells were deterministically trapped into the TW1 (Fig. 3E). The inherent cell trapping capability of each trap-well was evaluated by trapping cancer cells. The trapping efficiency is affected by various experimental parameters, including flow rate for cell delivery, size of trap-wells, and electrical potential used to induce dielectrophoresis. Among these parameters, we selected electrical potential to evaluate the single-cell trapping capability of the trap-well. Various electrical potentials (10, 15, and 20 Vpp at 8 MHz) were applied to the electrodes. The ratio of microwells was calculated by counting the number of microwells containing 0, 1, and 2 cells from the image taken 10 minutes after trapping (Fig. 3F). For the low magnitude of electrical potential (10 Vpp), 55 ± 6.5% of microwells were occupied by single cells, but other microwells were empty. When the electrical potential was increased to 15 Vpp, 99 ± 0.9% of microwells were occupied by single cells. For the high electrical potential of 20 Vpp, all the trap-wells were occupied by cells, but multiple cells were trapped into the trap-wells due to the strong DEP force. In addition to electrical potential, the flow rate for delivering cells is also a critical parameter for single-cell trapping. In our device, the DEP force is highly localized around the SiO_2 trap-wells. Therefore, if the flow velocity for cell delivery increases, the cells have a shorter exposure time to the electric fields for

DEP as they flow over the trap-wells. Additionally, higher flow velocity results in stronger Stokes' drag forces on the cells, making it difficult to trap them stably. Conversely, a flow rate that is too slow may lead to multiple cells being trapped and prolonged trapping times. Therefore, a balance between flow rate and electrical potential must be considered to achieve efficient single-cell trapping.

Highly efficient deterministic single-cell trapping has been successfully demonstrated with the SiO_2 trap-wells. Since the trap-wells were formed by etching the SiO_2 passivation layer, electric fields were formed inside of the trap-wells and the electric fields were efficiently blocked by the passivation layer between trap-wells. Moreover, the tiny electrodes aligned with the trap-wells allow the formation of a highly localized electric field inside of trap-wells. These highly localized electric fields and cell-sized trap-wells allow deterministic single-cell trapping with high efficiency. Since the ability of single-cell trapping with a very high occupancy ratio of the trap-well is highly reliant on the diameter of the trap-well, adjustment of the size of the trap-well is required for the trapping of different sizes of cells.

Single cell trapping into designated trap-wells

To investigate the inherent trapping efficiency of each trap-well, the single-cell occupancy ratio for each trap-well was investigated by trapping PC3 cells with electrical potentials of 10 Vpp or 15 Vpp. The PC3 cells were introduced into the device and trapped into TW1, TW2, or TW3 by applying the electrical potentials to electrode 1 (E1), electrode 2 (E2), or electrode 3 (E3), respectively. The single cells were trapped into the designated positions of the trap-wells, and no cells were trapped in unwanted positions of the trap-wells (Fig. 4A). After 5 minutes from DEP trapping, the fluorescence image of the trap-well array was acquired, and the number of trap-wells containing zero, one, or two cells was counted. The single-cell occupancy ratio was calculated from the percentage ratio of the number of trap-wells containing a single cell to the total number of trap-wells. For the electric potential of 10 V, the single-cell occupancy ratio was 55 ± 7%, 59 ± 19%, and 51 ± 7% for TW1, TW2, and TW3, respectively. The device showed a very high single-cell occupancy ratio for each trap-well with the electrical potentials of 15 V; 99 ± 1%, 96 ± 2%, and 99 ± 1% for TW1, TW2, and TW3, respectively (Fig. 4B). There was no significant difference in the single-cell occupancy ratio for each trap-well.

The SiO_2 trap-wells showed a very high single-cell occupancy ratio, and the cells were trapped in the designated positions of the trap-wells with very high efficiency. The single cells were successfully trapped in the designated positions of the trap-wells because the interconnection

of the electrodes allows control of the electrodes of each group of trap-wells. Moreover, highly localized electric fields formed on the trap-well allow trapping cells in the designated positions of the trap-wells; no cells were trapped in the unwanted trap-wells because the electric field was efficiently insulated by SiO_2 passivation layers. Such precise control of single-cell trapping allows efficient pairing or combination of single cells in the combinatorial reactors.

Pairing of single cells

The feasibility of the device was demonstrated by pairing different populations of cells at the single-cell level. Two different groups of human prostate cancer cell lines (PC3) stained with Calcein (green-PC3) or Calcein Red-Orange (red-PC3) were trapped using the combinatorial reactor sequentially. First, green-PC3 cells were introduced into the microfluidic device and trapped in trap-well-1 (TW1) by applying electrical potential to E1, which is aligned with TW1. After washing out the remaining green-PC3 cells, red-PC3 cells were introduced into the device and trapped in trap-well-2 (TW2) by applying electrical potential to the electrodes of E2, which is aligned with TW2, while E1 was kept on to hold previously trapped green-PC3 cells. After cell trapping, green and red fluorescence images were taken with appropriate filter sets for imaging green-PC3 and red-PC3 cells, respectively (Fig. 5). The weak fluorescence from red-PC3 cells appeared in the green channel because the Calcein Red-Orange used for red-PC3 cell staining can be excited by the green channel filter and emit weak green fluorescence. However, no green-PC3 cells were imaged in the red fluorescence channel. From the fluorescence image, the pairing efficiency was calculated as the percentage ratio of the number of combinatorial wells containing single green-PC3 and red-PC3 cells to the number of CRs in the image. The DSCR shows a very high pairing efficiency of 93 ± 2%. Compared to a previous single-cell pairing device that used multiple electrodes on the top and bottom surfaces of microfluidic devices, which achieved a pairing success rate of 44%[29], the DSCR shows a very high single cell pairing efficiency since SiO_2 trap-well allows highly deterministic single-cell trapping during sequential pairing process.

Efficient pairing of single cells was successfully demonstrated by sequentially trapping each cell population in designated trap-wells using interconnected electrodes. The most important function for single-cell pairing is a high single-cell occupancy ratio. During the cell pairing process, the red-PC3 cells were trapped in TW2 but not in TW1 since TW1 was already occupied by green-PC3 cells. On the other hand, when vacant TW1 existed, the red-PC3 cells would be trapped in the vacant TW1. Then, two red-PC3 cells would be trapped in the same combinatorial microwell. When the trap-wells were vacant or multiple cells were trapped, the second population

of cells would be trapped in the first trap-well. Hence, a very high single-cell occupancy ratio is important for pairing single cells, which was achieved using cell-sized trap-wells fabricated by the SiO_2 passivation layers and highly localized electric fields for DEP trapping in the DSCR.

Combination of multiple single cells

The feasibility of combining multiple single cells was demonstrated by sequentially trapping three different groups of PC3 cells, stained with Calcein (green-PC3), Calcein Red-Orange (red-PC3), and Hoechst (blue-PC3), into a deterministic single-cell trapping device (DSCR). Green-PC3 cells were introduced into the microfluidic device and trapped in trap-well-1 (TW1) by applying an electrical potential to electrode E1 located at the bottom of TW1. After washing out the remaining cells, red-PC3 cells were introduced and trapped in trap-well-2 (TW2) by applying an electrical potential to electrode E2 located at the bottom of TW2, while TW1 was kept active to hold the previously trapped green-PC3 cells. Red-PC3 cells were successfully trapped in TW2 but not in TW1, which was already occupied by green-PC3 cells. Finally, after washing out the remaining cells, blue-PC3 cells were introduced and trapped in trap-well-3 (TW3) by applying an electrical potential to electrode E3 located at the bottom of TW3, while TW1 and TW2 were kept active to retain the previously trapped green-PC3 and red-PC3 cells.

Figure 6 shows a merged fluorescence image of the trapped cells, captured using appropriate filter sets for each cell population at the same location. The weak fluorescence from green-PC3 and red-PC3 cells appeared in the blue channel, while the weak fluorescence from red-PC3 cells appeared in the green channel, confirming that different cell types were trapped in the respective trap-wells. The combination efficiency was calculated as the percentage ratio of the number of trap-wells containing single green-PC3, red-PC3, and blue-PC3 cells to the total number of trap-wells. The DSCR demonstrated a high combination efficiency of 82 ± 7%.

The deterministic combination of three different cell populations at the single-cell level was successfully achieved by sequentially trapping each population into designated trap-wells. The high single-cell occupancy ratio and individual control of trap-wells allowed for precise trapping of each cell type. While water-in-oil droplets can also be used for combining multiple single cells by adjusting the concentration to one cell per droplet, the maximum efficiency for combining three different cell populations using statistical methods would be less than 3% according to Poisson statistics. This statistical limitation was overcome in the present study by deterministically trapping each population of cells into the SiO_2 trap-wells. The number of different cell populations for combination can be increased by adding more trap-wells into CR.

This is easily achieved by expanding the size of the CR and incorporating additional trap-wells within them, with individual electrode control enabled by the multilayer interconnected electrodes.

Conclusion

In this report, we present a microfluidic device implemented on a Si/SiO_2 structure for the deterministic combination of multiple cell populations at the single-cell level. The highly localized electric fields in each trap-well and the individual control of electrodes enable the sequential trapping of each population of single cells into designated locations. We believe that the DSCR can be effectively used for pairing single cells or compartmentalizing multiple single cells, thereby overcoming the limitations of Poisson distribution in pairing or combination efficiency. The deterministic combination of single cells using the DSCR will facilitate the analysis of multiple cell-cell communications at the single-cell level and enable the indexing of single cells by trapping each cell with barcoded beads, which can be used for single-cell transcriptome analysis.

Acknowledgements

This work was supported by JST PRESTO Grant Number JPMJPR17H3, and by JSPS KAKENHI Grant Numbers JP23H03865, JP24K03302.

References

1. E. Z. Macosko, A. Basu, R. Satija, J. Nemesh, K. Shekhar, M. Goldman, I. Tirosh, A. R. Bialas, N. Kamitaki, E. M. Martersteck, J. J. Trombetta, D. A. Weitz, J. R. Sanes, A. K. Shalek, A. Regev and S. A. McCarroll, *Cell*, 2015, **161**, 1202-1214.
2. A. M. Klein, L. Mazutis, I. Akartuna, N. Tallapragada, A. Veres, V. Li, L. Peshkin, D. A. Weitz and M. W. Kirschner, *Cell*, 2015, **161**, 1187-1201.
3. Y. H. Cheng, Y. C. Chen, E. Lin, R. Brien, S. Jung, Y. T. Chen, W. Lee, Z. Hao, S. Sahoo, H. Min Kang, J. Cong, M. Burness, S. Nagrath, S. W. M and E. Yoon, *Nat Commun*, 2019, **10**, 2163.
4. Y. Zhou, N. Shao, R. Bessa de Castro, P. Zhang, Y. Ma, X. Liu, F. Huang, R. F. Wang and L. Qin, *Cell Rep*, 2020, **31**, 107574.
5. X. Tang, X. Liu, P. Li, F. Liu, M. Kojima, Q. Huang and T. Arai, *Analytical chemistry*, 2020, **92**, 11607-11616.
6. L. Li, H. Wang, L. Huang, S. A. Michael, W. Huang and H. Wu, *Analytical chemistry*,

2019, **91**, 15908-15914.

7. F. A. Shaik, C. Lewuillon, A. Guillemette, B. Ahmadian, C. Brinster, B. Quesnel, D. Collard, Y. Touil, L. Lemonnier and M. C. Tarhan, *Lab on a chip*, 2022, **22**, 908-920.
8. A. Desalvo, F. Bateman, E. James, H. Morgan and T. Elliott, *Lab on a chip*, 2020, **20**, 3772-3783.
9. A. I. Segaliny, G. Li, L. Kong, C. Ren, X. Chen, J. K. Wang, D. Baltimore, G. Wu and W. Zhao, *Lab on a chip*, 2018, **18**, 3733-3749.
10. Y. Li, J. H. Jang, C. Wang, B. He, K. Zhang, P. Zhang, T. Vu and L. Qin, *Adv Biosyst*, 2017, **1**, e1700085.
11. B. Dura, M. M. Servos, R. M. Barry, H. L. Ploegh, S. K. Dougan and J. Voldman, *Proceedings of the National Academy of Sciences of the United States of America*, 2016, **113**, E3599-3608.
12. J. R. Rettig and A. Folch, *Analytical chemistry*, 2005, **77**, 5628-5634.
13. D. Di Carlo, L. Y. Wu and L. P. Lee, *Lab on a chip*, 2006, **6**, 1445-1449.
14. D. Di Carlo, N. Aghdam and L. P. Lee, *Analytical chemistry*, 2006, **78**, 4925-4930.
15. S. H. Kim, T. Yamamoto, D. Fourmy and T. Fujii, *Small*, 2011, **7**, 3239-3247.
16. M. He, J. S. Edgar, G. D. Jeffries, R. M. Lorenz, J. P. Shelby and D. T. Chiu, *Analytical chemistry*, 2005, **77**, 1539-1544.
17. H. Hu, D. Eustace and C. A. Merten, *Lab on a chip*, 2015, **15**, 3989-3993.
18. R. H. Cole, S. Y. Tang, C. A. Siltanen, P. Shahi, J. Q. Zhang, S. Poust, Z. J. Gartner and A. R. Abate, *Proceedings of the National Academy of Sciences of the United States of America*, 2017, **114**, 8728-8733.
19. H. Chai, Y. Feng, F. Liang and W. Wang, *Lab on a chip*, 2021, **21**, 2486-2494.
20. C. K. He, Y. W. Chen, S. H. Wang and C. H. Hsu, *Lab on a chip*, 2019, **19**, 1370-1377.
21. K. Kamiya, Y. Abe, K. Inoue, T. Osaki, R. Kawano, N. Miki and S. Takeuchi, *Adv Healthc Mater*, 2018, **7**, e1701208.
22. B. Dura, S. K. Dougan, M. Barisa, M. M. Hoehl, C. T. Lo, H. L. Ploegh and J. Voldman, *Nat Commun*, 2015, **6**, 5940.
23. K. Zhang, C. K. Chou, X. Xia, M. C. Hung and L. Qin, *Proceedings of the National Academy of Sciences of the United States of America*, 2014, **111**, 2948-2953.
24. B. Dura, Y. Liu and J. Voldman, *Lab on a chip*, 2014, **14**, 2783-2790.
25. L. Fan, Z. Guan, T. Luo, J. Ren, R. H. W. Lam and D. Sun, *Biomicrofluidics*, 2021, **15**, 054103.

26. Z. Guan, S. Jia, Z. Zhu, M. Zhang and C. J. Yang, *Analytical chemistry*, 2014, **86**, 2789-2797.
27. Y. J. Yamanaka, C. T. Berger, M. Sips, P. C. Cheney, G. Alter and J. C. Love, *Integr Biol (Camb)*, 2012, **4**, 1175-1184.
28. C. Wu, R. Chen, Y. Liu, Z. Yu, Y. Jiang and X. Cheng, *Lab on a chip*, 2017, **17**, 4008-4014.
29. M. Sen, K. Ino, J. Ramon-Azcon, H. Shiku and T. Matsue, *Lab on a chip*, 2013, **13**, 3650-3652.
30. W. He, L. Huang, Y. Feng, F. Liang, W. Ding and W. Wang, *Biomicrofluidics*, 2019, **13**, 054109.
31. S. H. Kim and T. Fujii, *Lab on a chip*, 2016, **16**, 2440-2449.
32. J. Park, C. Park, Y. Sugitani, T. Fujii and S. H. Kim, *Lab on a chip*, 2022, **22**, 3000-3007.
33. D. Lee, D. Jung, F. Jiang, G. V. Junek, J. Park, H. Liu, Y. Kong, A. Wang, Y. Kim, K. S. Choi, J. Wang and H. Wang, *IEEE Trans Biomed Circuits Syst*, 2023, **17**, 1214-1226.
34. M. Punjiya, A. Mocker, B. Napier, A. Zeeshan, M. Gutsche and S. Sonkusale, *Biosens Bioelectron*, 2020, **150**, 111931.
35. M. Di Trapani, N. Manaresi and G. Medoro, *Cytometry A*, 2018, **93**, 1260-1266.
36. H. Zhang, P. Wang, N. Huang, L. Zhao, Y. Su, L. Li, S. Bian and M. Sawan, *Front Bioeng Biotechnol*, 2023, **11**, 1258626.
37. F. T. Jaber, F. H. Labeed and M. P. Hughes, *J Neurosci Methods*, 2009, **182**, 225-235.

Contact

* S. H. Kim; shkim@iis.u-tokyo.ac.jp

Figure Legends

Figure 1. Schematic illustration of deterministic combinatorial single-cell reactor. (A) Different population of single cells were trapped into individual reactors. (B) Schematic illustration of microfluidic device coupled with Si/SiO_2 structure. The combinatorial reactor contains tree trap-wells. The cell-sized trap-well allows highly efficient single cell trapping. The electrodes below the trap-well induce highly localized electric fields. (C) Schematic illustration of the sequential trapping of single cells for combination of three different population of single cells. The green cells were introduced into the microfluidic device and trapped into TW1 by applying electrical potential into the E1. After washing remained cells, next population of cells were introduced into the device and trapped into the TW2 by applying electrical potential to E2. Finally, third population of cells were trapped into TW3.

Figure 2. Addressable electroactive trap-wells. (A) Fabricated addressable electroactive trap-wells in an array. The SiO_2 trap-well was aligned with a pair of electrodes in a reactor, with each electrode individually connected to its respective transistor. (B) Cross-sectional view of SEM image of a SiO_2 trap-well. Scale bar is 5 μm. (C) Simulated electric field distribution and vectors of the electric field gradient ($\nabla|\boldsymbol{E}|^2$) for without trap-well (left) and with trap-well (right). Electric potentials were assigned at the electrode boundaries. White lines indicate the surface of SiO_2 layer. The $\nabla|\boldsymbol{E}|^2$ vectors were directed towards the electrodes and the magnitude of $\nabla|\boldsymbol{E}|^2$ was significantly increased with trap-well. (D) Selective trapping of single cells using addressable electroactive trap-wells (a part of the Supplementary Movie 1). An electrical potential of 10 Vpp at 8 MHz was applied to the selected trap-wells (yellow dotted circles). Scale bars are 100 μm. (E) Selective release of trapped cells (a part of the Supplementary Movie 2). After trapping PC3 cells by activating all trap-wells with an electrical potential of 10 Vpp at 8 MHz, selected trap-wells were deactivated, and the cells in those wells were immediately released. However, cells in the still-activated trap-wells, indicated by yellow dotted circles, were not released. Scale bars are 100 μm.

Figure 3. Single cell trapping using DSCR. (A) Fabricated DSCR coupled with microfluidic channel. The Si/SiO_2 structure was permanently bonded with PDMS microfluidic channel. Reservoir for cell loading was connected with the inlet of the microfluidic channel and the outlet of the microfluidic channel is connected with the syringe. The device contains array of combinatorial reactors. Scale bar is 100 μm. (B) Combinatorial reactor. The combinatorial reactor

contains three trap-wells. The electrodes are aligned with the CR. Scale bar is 100 μm. (C) Schematic illustration of electrical circuit of the electrodes. Each trap-well contains pair of electrodes. One electrode was connected with ground, and the power source was connected with the counter electrodes. (D) Time lapse image of single cell trapping using DSCR. The cells were trapped into TW1 when the electrical potential was applied to E1. Only single cells were trapped into TW1. Yellow arrow head indicates the cells flowing over the DSCR and trapped into TW1. Scale bar is 100 μm. (E) Array of trapped single cells. Single cells were trapped into TW1. No cells were trapped into TW2 or TW3. Scale bar is 100 μm. (F) Ratio of trap-wells contains 0, 1 or 2 cells versus electrical potential applied to the electrodes for DEP trapping.

Figure 4. Single cells trapped into designated trap-wells. (A) Fluorescence images of trapped single cells into designated trap-wells. The PC3 cells were trapped into TW1, TW2, or TW3, respectively. Scale bar is 100 μm. (B) Single occupancy ratio with respect to each trap-well. The percentage ratio of the number of trap-wells containing a single cell to the total number of trap-wells was calculated after cell trapping with electric potential of 10 V and 15 V.

Figure 5. Fluorescence images of paired single cells. The green-PC3 cells were trapped into TW1 and then the red-PC3 cells were trapped into TW2. Fluorescence images were acquired after cell trapping with appropriate filter sets for each cell population at the same location and the fluorescence images were merged. Scale bar is 100 μm.

Figure 6. Fluorescence images of combination of single cells. The green-PC3, red-PC3 and blue-PC3 cells were trapped into TW1, TW2 and TW3 sequentially. Fluorescence images were acquired after trapping with appropriate filter sets for each cell population at the same location and the fluorescence images were merged. Scale bar is 100 μm.

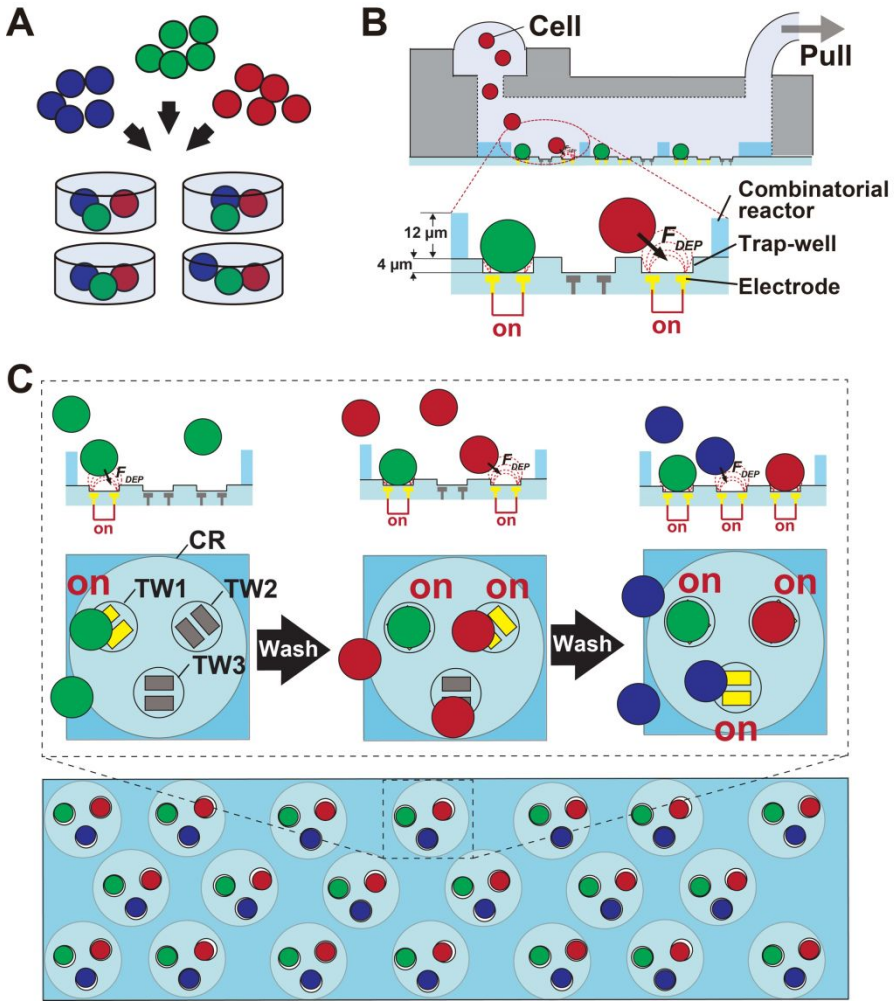
A
B
Cell
Pull
Combinatorial reactor
12 μm
4 μm
F_{DEP}
Trap-well
Electrode
on
on
C
F_{DEP}
on
CR
TW1
TW2
TW3
Wash
Wash

Fig. 1

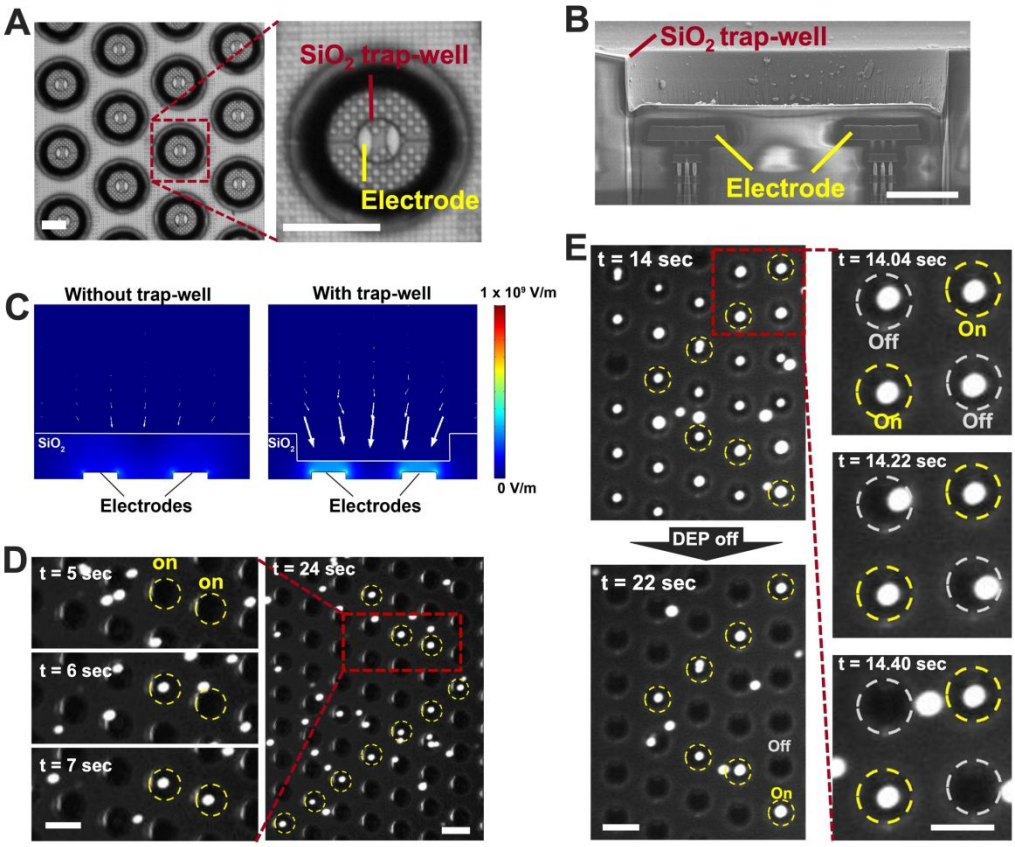
A
SiO2 trap-well
Electrode
B
SiO2 trap-well
Electrode
C
Without trap-well
With trap-well
1 x 10⁹ V/m
0 V/m
SiO2
Electrodes
D
t = 5 sec
on
t = 6 sec
t = 7 sec
t = 24 sec
E
t = 14 sec
t = 14.04 sec
Off
On
t = 14.22 sec
t = 14.40 sec
DEP off
t = 22 sec
Off
On

Fig. 2

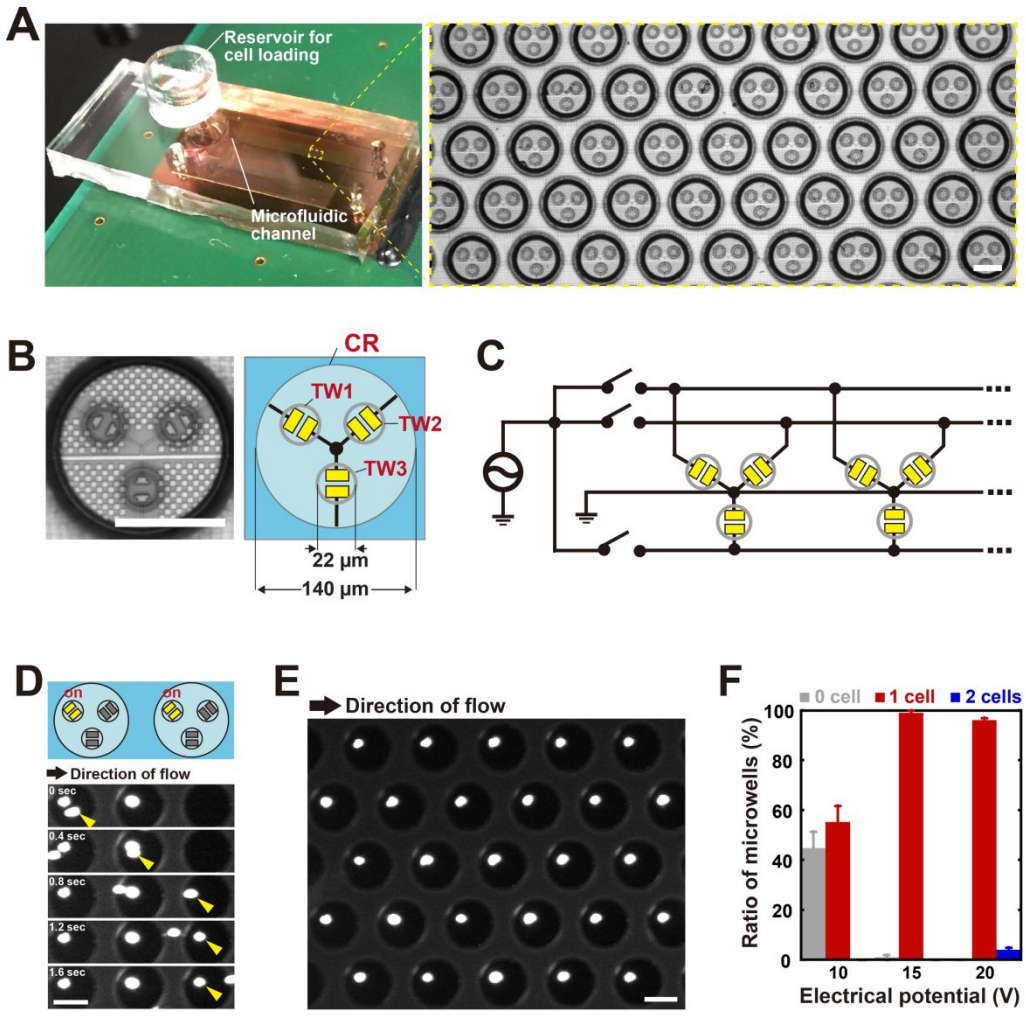
A
Reservoir for cell loading
Microfluidic channel
B
CR
TW1
TW2
TW3
22 μm
140 μm
C
D
on
on
Direction of flow
0 sec
0.4 sec
0.8 sec
1.2 sec
1.6 sec
E
Direction of flow
F
0 cell
1 cell
2 cells
Ratio of microwells (%)
100
80
60
40
20
0
10
15
20
Electrical potential (V)

Fig. 3

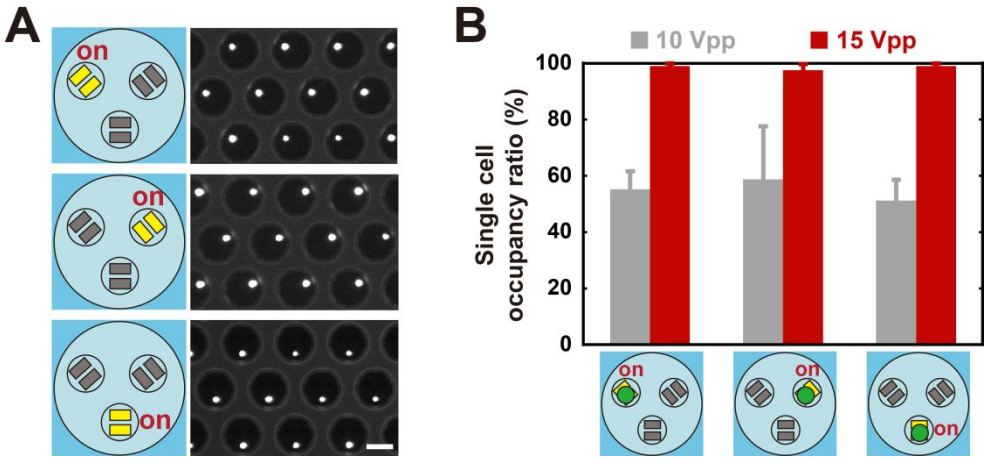
A
on
on
on
B
10 Vpp
15 Vpp
Single cell occupancy ratio (%)
100
80
60
40
20
0
on
on
on

Fig. 4

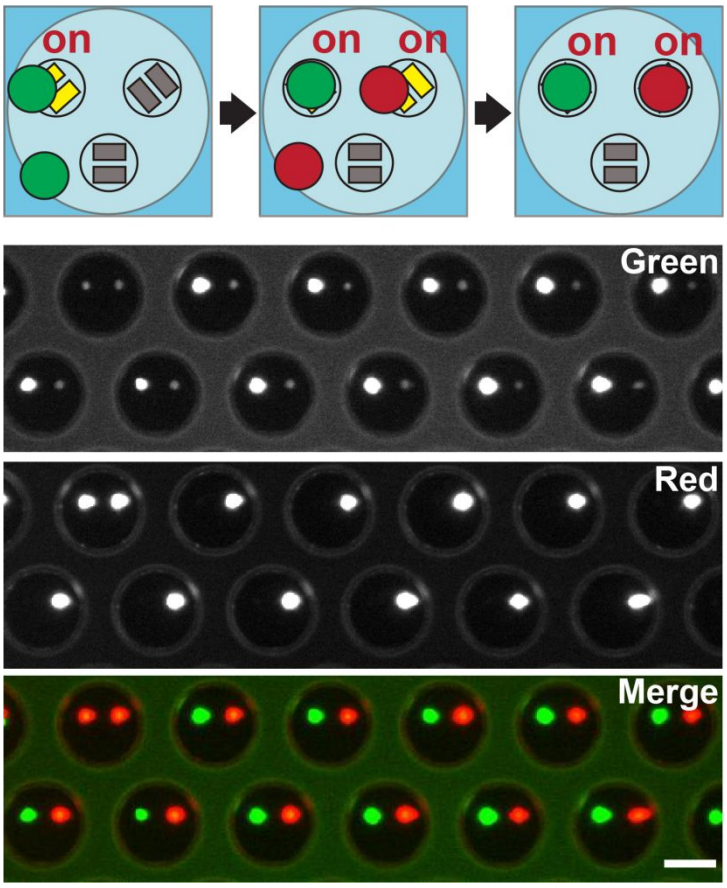

Fig. 5

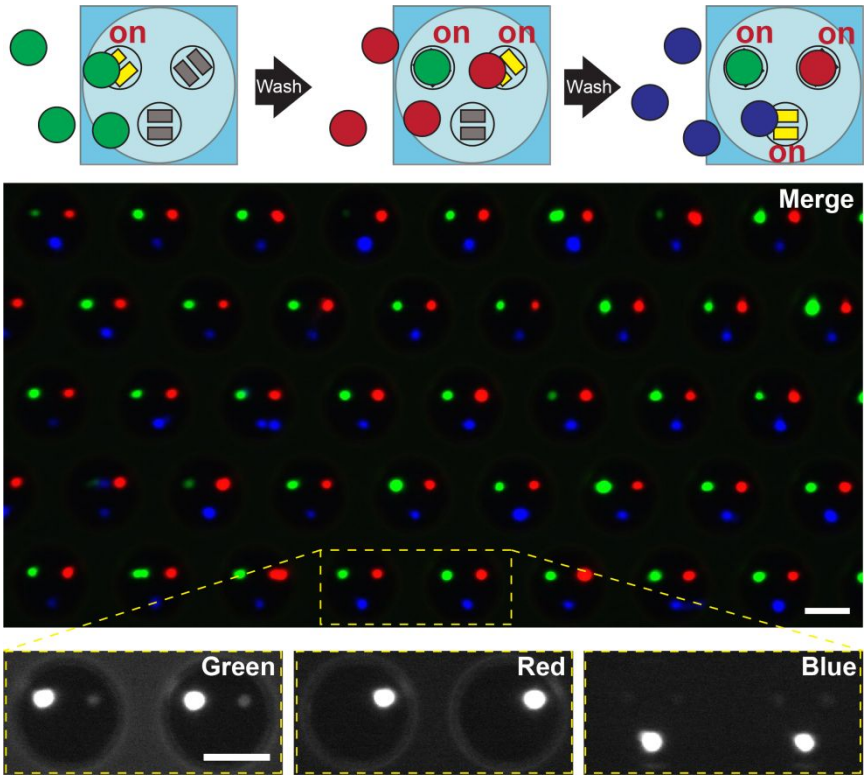

Fig. 6

Highly efficient combination of multiple single cells using deterministic single-cell combinatorial reactor

Mina Yoshida[1], Saori Tago[1], Kunihiko Iizuka[1,2], Teruo Fujii[1] and Soo Hyeon Kim[1*]

[1] Institute of Industrial Science, University of Tokyo, Tokyo, Japan

[2] Lab Arco Limited, Osaka, Japan

The data supporting this article have been included as part of the Supplementary Information.